Journal Pre-proof

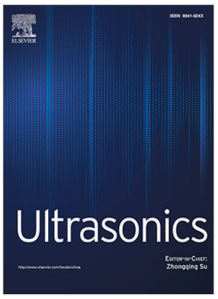

The effects of dispersion on time-of-flight acoustic velocity measurements in a wooden rod

Adli Hasan Abu Bakar, Mathew Legg, Daniel Konings, Fakhrul Alam

PII: S0041-624X(22)00218-9
DOI: https://doi.org/10.1016/j.ultras.2022.106912
Reference: ULTRAS 106912

To appear in: *Ultrasonics*

Received date : 8 August 2022
Revised date : 9 November 2022
Accepted date : 2 December 2022

Please cite this article as: A.H.A. Bakar, M. Legg, D. Konings et al., The effects of dispersion on time-of-flight acoustic velocity measurements in a wooden rod, *Ultrasonics* (2022), doi: https://doi.org/10.1016/j.ultras.2022.106912.

The Effects of Dispersion on Time-of-Flight Acoustic Velocity Measurements in a Wooden Rod

Adli Hasan Abu Bakar, Mathew Legg*, Daniel Konings, Fakhrul Alam

Department of Mechanical and Electrical Engineering, Massey University, Auckland, New Zealand

Abstract

The stiffness of wood can be estimated from the acoustic velocity in the longitudinal direction. Studies have reported that stiffness measurements obtained using time-of-flight acoustic velocity measurements are overestimated compared to those obtained using the acoustic resonance and bending test methods. More research is needed to understand what is causing this phenomenon. In this work, amplitude threshold time-of-flight, resonance, and guided wave measurements are performed on wooden and aluminium rods. Using guided wave theory, it is shown through simulations and experimental results that dispersion causes an overestimation of time-of-flight measurements. This overestimation was able to be mitigated using dispersion compensation. However, other guided wave techniques could potentially be used to obtain improved measurements.

Keywords: Wood, aluminium, rod, ToF, guided waves, amplitude threshold.

1. Introduction

The measurement of the mechanical properties of wood such as stiffness is important for the forestry industry. The stiffness of wood can be used as a metric to segregate logs into different grades. This can help maximise the profitability and sustainability within the wood industry [1]. The stiffness of timber may be measured using static bending tests, which are considered to be the gold standard. However, ideally, the properties of the wood should be known before it is processed to ensure it is suitable for the end product [2]. Non-Destructive Testing (NDT) techniques [3, 4] have been developed to determine the properties of wood before processing and without damaging them.

The main NDT technique used to measure the stiffness of wood is acoustics since it is simple to use and inexpensive compared to other methods. Wood is an orthotropic material meaning that the mechanical properties are independent in three orthogonal axes. For wood, the acoustic velocity in the longitudinal

*Corresponding author

Email addresses: A.Hasan@massey.ac.nz (Adli Hasan Abu Bakar), M.Legg@massey.ac.nz (Mathew Legg), D.Konings@massey.ac.nz (Daniel Konings), F.Alam@massey.ac.nz (Fakhrul Alam)

direction v_l is often described by

$$v_l = \sqrt{\frac{E_L}{\rho}}, \tag{1}$$

where ρ is the density of the material and E_L is the Modulus of Elasticity (MoE) in the longitudinal direction. The MoE in the longitudinal direction is commonly used to describe the stiffness of wood. This equation is based on fundamental 1D wave theory [5] which does not include factors that can affect the acoustic velocity such as temperature, moisture content, presence of knots, Poisson's ratios and variation in grain angle [6]. There are more complex models for wood which include some of these factors [7, 8]. For example, Legg & Bradley [6] provide a model that includes orthotropic Poisson's ratios. However, the 1D wave theory given in Eqn. 1 is predominantly used in the literature related to wood stiffness. The two most commonly used acoustic methods to measure the stiffness of wood are the resonance and Time of Flight (ToF) methods, as described below. The resonance method can be used on felled logs, while the ToF method can be used on both standing trees and felled logs.

1.1. Acoustic methods and overestimation

The resonance method involves generating longitudinal stress waves by performing a hammer hit at one end of the sample in the direction parallel to the grain. A Fast Fourier Transform (FFT) is performed on the received acoustic signal and resonance frequencies are identified. The longitudinal resonance acoustic velocity can then be calculated using

$$v_{res} = \frac{2Lf_n}{n}, \tag{2}$$

where L is the length of the sample, f_n is the n^{th} resonant frequency and $n = 1, 2, 3\ldots$. Note that flexural resonance techniques have also been used by researchers where the hammer hit is impacted normal to the grain [9].

For wood related studies, the ToF method generally involves two probes which are inserted into a sample separated by a distance d. The acoustic velocity can be calculated using

$$v_{tof} = \frac{d}{T}, \tag{3}$$

where T is the propagation time of a stress wave from one probe to the other. Traditionally, a hammer hit is performed at or near one of the probes to generate longitudinal stress waves. Hammer hit excitation is generally used for NDT measurements of wood properties because it provides a strong excitation signal with a good Signal-to-Noise Ratio (SNR). This is important given the highly attenuative nature of wood, particularly at higher acoustic frequencies. In addition to hammer hit excitation, ultrasonic excitation signals are also used for acoustic velocity measurements in wood [10].

In wood studies, the propagation time T is predominantly obtained by measuring the First Time of Arrival (FToA) of the signal at each receiver probe. For hammer hit excitation, signal peaks are not

commonly used as they can be distorted during propagation, which can lead to large errors. The FToA technique identifies when the signal is first detected at each of the receiver probes and ignores the remainder of the signal. The amplitude threshold method appears to be the main technique used in wood studies to determine the FToA of the received signal. The method is also widely used in ultrasonic NDT to determine the FToA of a propagating signal in order to extract the ToF. This technique measures the time when the signal at each receiver first goes above a chosen threshold value [11, 12, 13]. Alternatively, other FToA methods such as Akaike Information Criterion (AIC) [14], Modified Energy Ratio (MER) [15] and cross-correlation [16] have also been used.

Stiffness measurements obtained using acoustic resonance and ToF have shown good correlations with those obtained using static bending tests. However, the ToF method results have a systematic overestimation in stiffness measurements compared to the values obtained using both static bending tests and resonance. This overestimation is related to the ToF method measuring acoustic velocities which are systematically higher than those obtained using acoustic resonance [6].

Several studies have suggested possible reasons as to why this is occurring. For example, the variation in stiffness from pith to bark [17], the age and diameter of the trees and the difference in wave propagation of the acoustic signals used in the two methods [5]. Despite these suggestions, the exact cause of the overestimation is still not known.

1.2. Guided waves and dispersion effects

For rod-like structures, guided waves are expected to propagate as different types of vibrations, which are called wave modes [6]. Unlike 1D wave theory, guided wave theory considers the dispersion of wave modes. Dispersion is influenced by the mechanical properties and diameter of a sample. Dispersion is caused by the propagation of different frequency components at different velocities. This causes the signal to spread out as it propagates through a medium [18].

Guided wave NDT testing techniques have been used to measure wood properties [19, 20]. However, this is an emerging area of research and there have been relatively few studies on this topic. In our previous paper [21], a 2D FFT method was used to obtain wavenumber-frequency domain dispersion curves for wood and aluminium rod samples. These dispersion curves showed the presence of the fundamental longitudinal, flexural and torsional wave modes in the rod samples. The resonance velocity was found to roughly correlate with the L(0,1) wave mode dispersion curve at low frequencies. However, phase velocities were not calculated from these wavenumber-frequency domain plots since the resulting phase velocities would have had high errors due to the low resolution associated with the 2D FFT method.

Generally, in guided wave testing, ultrasonic transducers are used to generate narrowband excitation signals to reduce the effects of dispersion and limit the number of wave modes excited [22, 23]. Hammer hits or sharp impacts are therefore generally not used in guided wave testing since they generate wide bandwidth

excitation signals and provide less control. This means that there are a limited number of studies on dispersion and guided waves for impact-like excitation.

The Split Hopkinson Pressure Bar (SHPB) is a technique that measures the dynamic mechanical behaviour of materials, particularly at high strain rates, by analysing the shape of signals generated by a sharp impact [24]. Knowledge of guided waves and dispersion has been used to improve the accuracy of these measurements. It has been reported that dispersion can cause signal distortion on SHPB tests on metal samples. This can cause significant changes to the rise time at the start of the measured impact signal [25].

Although the SHPB technique does not use velocity measurements, the findings from this area of research could provide some insights into a potential cause of error in ToF measurements obtained using FToA techniques such as amplitude thresholding. Could the distortion caused by dispersion at the start of the signal affect the accuracy of amplitude threshold ToF velocity measurements?

For the SHPB technique, dispersion compensation methods have been developed to mitigate dispersion effects which have helped to reduce signal distortion and improve the rise time at the start of the signal to give more accurate results [26, 27, 28]. Besides the SHPB technique, dispersion compensation techniques have also been used to reduce the effects of dispersion on ultrasonic guided wave measurements on metal samples [29, 30, 31]. One of these studies, which was performed by Xu et al. [32], has investigated the effect of dispersion compensation on ToF measured values for ultrasonic guided waves. However, these ToF measurements were not obtained using FToA techniques. Instead, the ToF measurements were obtained by measuring the propagation time of the largest peak at the centre of the wave packet for different propagation distances. They reported that more accurate group velocity ToF measurements were obtained after dispersion compensation was performed.

No previous work has been found that has investigated the effect of dispersion on ToF measurements obtained using FToA methods (looking at the start of the signal, not the peak). Additionally, no studies have been found which have utilised dispersion compensation to reduce dispersion effects for acoustic measurements made on wood.

In this study, resonance, amplitude threshold ToF and guided wave longitudinal velocity measurements were performed on thin cylindrical aluminium and wooden rods. The amplitude threshold ToF acoustic velocities were measured before and after dispersion compensation was performed. The results were then compared with acoustic resonance velocities.

1.3. Contributions

The research presented here offers the following contributions. To the best of the author's knowledge, this is the first work to:

(1) Investigate the effects of dispersion on ToF acoustic velocity measurements made using the FToA.

(2) Show that dispersion effects can be a source of overestimation in FToA ToF velocity measurements.

(3) Use dispersion compensation to mitigate the overestimation in the measured FToA ToF velocity measurements. We are not aware of any previous studies that have performed dispersion compensation for wood.

The remainder of the paper is organised as follows. Section 2 describes the wave propagation and dispersion compensation theory. Section 3 describes the methodology, hardware and experimental procedure used. Section 4 presents the results obtained. Lastly, Section 5 provides a conclusion and suggestions for future work.

2. Wave propagation model

The following section outlines a simple wave propagation model that is used in this work to simulate the propagation of the sound waves through the wooden and aluminium rods. Also included is a description of the dispersion compensation technique used in this work. This allows the effects of dispersion on FToA acoustic velocity measurements to be evaluated.

Consider a signal $g(t)$ excited by a transducer, which only generates a single wave mode. The received signal $y(t)$ at a distance d from the transmitter can be modelled in the frequency domain as

$$Y(\omega) = G(\omega)e^{-j\ k(\omega)\ d\ -\ \alpha(\omega)\ d}, \tag{4}$$

where ω is the angular frequency, $G(\omega)$ is the Fourier transform of $g(t)$, $k(\omega)$ is the wavenumber, and $\alpha(\omega)$ is the attenuation [31]. The wave number can be calculated using

$$k = \frac{\omega}{v_{ph}}, \tag{5}$$

where v_{ph} is the phase velocity. The peak of the wave packet will propagate at the group velocity v_{gr}. For a narrowband signal, the distance and time t may be related using

$$d(t) = v_{gr}(\omega_o)\ t, \tag{6}$$

where ω_o corresponds to the central frequency of the narrow band excitation frequency.

For a dispersive material, both the phase and group velocity will be frequency-dependent resulting in dispersion. This causes the signal to spread out as it propagates. The above theory therefore allows dispersive guided wave propagation to be simulated using either theoretical or measured dispersion curves.

Dispersion compensation techniques have been developed to mitigate the effects of dispersion from the received guided wave signals in post-processing [29, 33, 34]. Consider that a received signal $y(t)$ has experienced dispersion. Dispersion compensation can be performed at the i_{th} propagation time t_i in the frequency domain using

$$\hat{Y}(\omega, t_i) = Y(\omega)e^{j(k(\omega)\ d(t_i) - w\ t_i)} \tag{7}$$

where $Y(\omega)$ is the Fourier transform of the received signal $y(t)$ and d is the propagation distance. This performs frequency domain shifting of each frequency component in the signal to correct for changes in phase velocity due to dispersion. Each frequency component of the signal is calculated using Equation 7 and the inverse Fourier transform

$$\hat{y}(t) = \text{IFFT}[\hat{Y}(\omega, t_i)], \tag{8}$$

is used to convert the frequency domain dispersion compensated signal to a time domain version. This will provide the correct dispersion compensation of the received signal $y(t)$ for a singe wave mode at time t_i but will over or under compensate for other times.

To correct the signal for all times, the above process can be performed in a loop, where the i_{th} iteration performs dispersion compensation for the i_{th} time in the signal. This value is saved into a new array, which is the dispersion compensated version of the received signal $y(t)$ for all times. This technique was used in this work to perform dispersion compensation. A more computationally efficient dispersion compensation method can be found in [29].

3. Methodology

3.1. Wood and aluminium rod samples

A radiata pine cylindrical rod with a diameter of 16 mm and a length of 2460 mm was used. The sample was chosen such that it did not have any observable defects. For comparison, measurements were repeated on a 6061-T6 aluminium cylindrical rod with a diameter of 16 mm and a length of 2510 mm. The aluminium sample is an isotropic and homogeneous material whose dispersion curves can be easily obtained since its mechanical properties are known. However, it should be noted that wood is orthotropic, inhomogenous and highly attenuative particularly at high frequencies.

Figure 1 shows the theoretical dispersion curves for a 16 mm diameter aluminium rod. The dispersion curves were obtained using GUIGUW [35]. The dispersion curves were obtained using the following parameters for a 16 mm diameter aluminium rod: Young's modulus = 68.9 GPa, density = 2,710 kg/m^3 and Poisson's ratio = 0.33. This would give a theoretical bulk wave speed of about 6175 m/s for the aluminium sample [6]. We can see that the three fundamental longitudinal, flexural and torsional wave modes are present. However, at higher frequencies or higher sample thickness, higher order wave modes are expected to be present.

3.2. Resonance setup

An 8 oz hammer with a metal head tip was used in the experiment to generate stress waves. For resonance measurements, a hammer hit parallel to the wood grain was performed at one exposed end of the sample to generate longitudinal stress waves. The resulting signal was measured using a GRAS 46BF-1 microphone

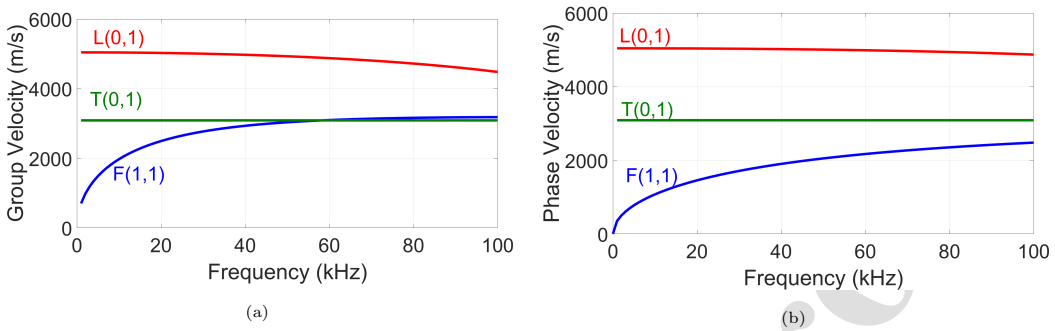

Figure 1: Theoretical dispersion curves for a 16 mm diameter aluminium rod showing the fundamental longitudinal L(0,1), torsional T(0,1) and flexural F(1,1) wave modes plotted as (a) group velocity and (b) phase velocity.

located at the opposite end of the sample relative to the hammer impact. The microphone was connected to a GRAS 26A-1 pre-amp and was powered through a GRAS 12AK power module. The received signal from the microphone was then sampled at 2 MHz using the Analog to Digital Converter (ADC) channels of a Data Translation DT9832 data acquisition module, see Figure 2. The received signal was saved to file and further processed in MATLAB.

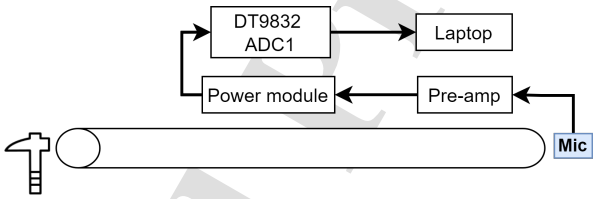

Figure 2: Experimental setup for resonance measurements

.

3.3. Hammer hit (ToF) setup

Traditionally, probes are inserted into a sample to penetrate through the bark and allow coupling of the acoustic signals to the wood. However, in this work we have used shear PZT transducers manufactured by TWI, UK [36] directly coupled to the wood sample by clamping them using springs, see Figure 3. This provides better control over the types of vibrations being measured and transmitted. For example, by aligning the transducers parallel to the grain, we can enhance the transmission and reception of longitudinal vibrations and suppress torsional and flexural vibrations [21, 37].

Two transducers were positioned as shown in Figure 4. The contact faces of the shear transducers were oriented parallel to the grain to enhance the reception of vibrations in the longitudinal direction. A hammer hit was performed at one end of the sample parallel to the grain. The received signal produced by the

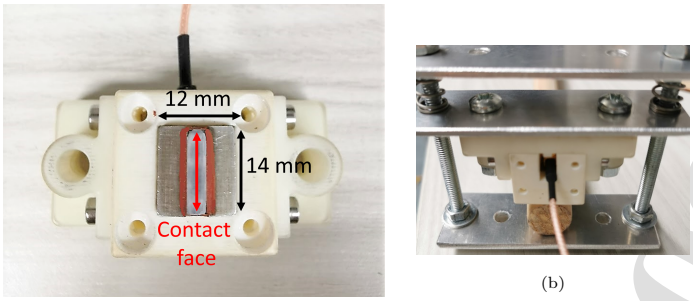

(a) (b)

Figure 3: Photo (a) shows one of the transducers used in this experiment. Photo (b) shows the transducer being pushed against a wooden rod sample using springs.

hammer hit has a high amplitude and hence pre-amps were not needed. The transducers were directly connected to the ADCs of the DT9832 and the received signal at RX1 and RX2 were sampled at 2 MHz and saved to file. The recording of the received signal was initiated by pressing a keyboard button just before a hammer hit was manually performed.

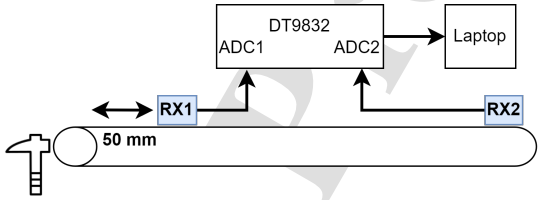

Figure 4: Experimental setup for hammer hit (ToF) measurement.

3.4. Tone burst and guided wave setup

Three shear transducers were positioned and clamped in the configuration shown in Figure 5. The contact faces of the transducers were oriented parallel to the grain to enhance the transmission and reception of vibrations in the longitudinal direction [21]. Note that the positioning of the RX1 and RX2 transducers was the same as for the hammer hit measurements.

The excitation signal applied to transducer TX was created in MATLAB and outputted from an Agilent 33210A Function Generator. To amplify the transmitted signal, a custom-built linear power amplifier capable of amplifying signals up to 400 Vpp was used. The receivers were connected to pre-amps and the received signal at RX1 and RX2 were sampled at 2 MHz using the ADC channels of the DT9832 module, refer Figure 5. The received signals were saved to file for further processing. In contrast to the manual hammer hit recordings, hardware triggering was used to synchronise the transmission of the transmit signal with the

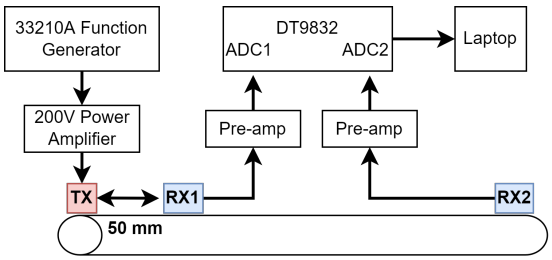

Figure 5: Experimental setup for tone burst and guided wave measurements.

recording of the received signal. Two types of excitation were made using this experimental setup, which are tone burst excitation with and without Hanning window.

Non-windowed tone burst measurements were used for amplitude threshold ToF measurement. These were used as they were narrowband and were more repeatable than hammer hit excitation. The tone bursts were five cycles of a 15 kHz sine wave. These measurements will be referred to as "tone burst measurements" in the following text.

Hanning-windowed tone bursts were used for the guided wave measurements. Windowing helps to reduce the bandwidth of the signal to minimise the effects of dispersion. These measurements used five cycles of a Hanning windowed sine wave with central frequencies ranging from 15 to 50 kHz in 1 kHz increments. These measurements were performed to experimentally measure the phase velocity dispersion curves for the L(0,1) wave mode and will be referred to as "guided wave measurements" in the remainder of the paper.

3.5. Data processing

For resonance measurements, the microphone recordings of hammer hits at the ends of the rods were processed to calculate resonance acoustic velocities for both samples. The FFT of the received signal was used to obtain the resonant frequencies. In most cases, the first or second harmonic is used to obtain the resonance velocity. However, reports in the literature have mentioned that resonance velocities vary depending on which harmonic frequency is used. Also, resonance measurements at lower frequencies are more prone to errors due to frequency resolution issues [38]. To minimise these errors, an average resonance velocity using the lowest five resonance frequency peaks using Equation 2 was obtained for each sample. This was repeated for five measurements and the average was taken as the resonance velocity. Figure 6 below shows the FFT spectra of the wood and aluminium samples obtained from the resonance measurement. The red-marked points correspond to the resonant peaks for the longitudinal wave mode.

ToF velocity measurements were obtained using the FToA amplitude threshold method. The times when the signal at receivers RX1 and RX2 first went above a certain threshold were measured. The difference between these times T was then calculated. The ToF velocity was then calculated using Equation 3. This was performed for both hammer impact and the 15 kHz sine wave tone bursts. The threshold was set to

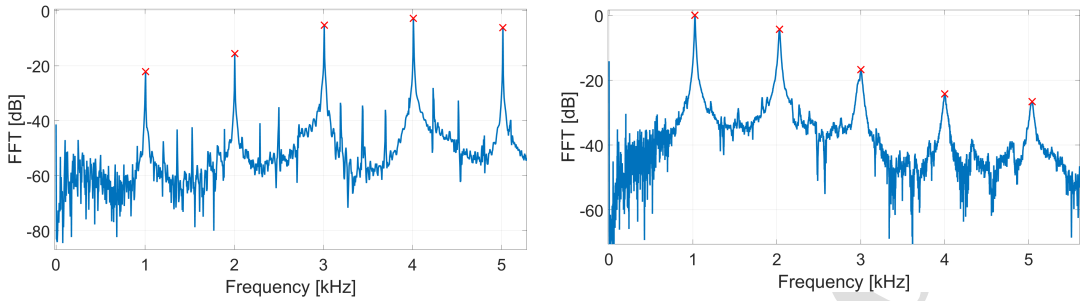

Figure 6: Plots of FFT spectra obtained from resonance measurements for (a) aluminium and (b) wood sample.

0.002 V and 0.02 V for the hammer impacts and tone bursts respectively. These values were chosen as they were approximately three times the standard deviation of the RMS of the noise and did not result in false positives. Note that a lower threshold value was used for the hammer hits as pre-amps were not used for these measurements which resulted in a lower noise. The average of five measurements was taken as the measured ToF acoustic velocity. The measurements were performed without removing the transducers.

Experimentally measured dispersion curves for the fundamental longitudinal L(0,1) wave mode were obtained from the guided wave measurements. These measurements were performed using Hanning windowed sine wave signals with varying transmit frequencies. Phase velocities were obtained from these measurements using a frequency-domain shifting technique. For each transmission, the received signal at RX1 was converted into the frequency-domain using the Fast Fourier Transform (FFT). Equation 4 was then used to simulate the propagation of the RX1 signal by a distance d using an initial phase velocity v_{ph}. The propagated signal was then converted back into the time-domain using the Inverse Fast Fourier Transform (IFFT). The Root Mean Squared Error (RMSE) between the propagated time-domain RX1 signal and the received signal at RX2 was calculated. The phase velocity was iteratively adjusted by 1 m/s until a minimum RMSE was obtained. The velocity value which corresponds to the minimum RMSE was taken as the phase velocity at the central transmit frequency. This process was repeated for a range of central transmit frequencies. Figure 7 shows a block diagram process of measuring the phase velocity from received signal RX1 and RX2.

3.6. Dispersion curves and dispersion compensation

Phase velocity dispersion curves were fitted using the calculated phase velocities of the guided wave measurements performed at various transmit frequencies for both samples. For the aluminium sample, a theoretical phase velocity dispersion curve of the L(0,1) wave mode was obtained using GUIGUW and the parameters mentioned in Section 3.1. The same could not be done for the wood sample as the mechanical

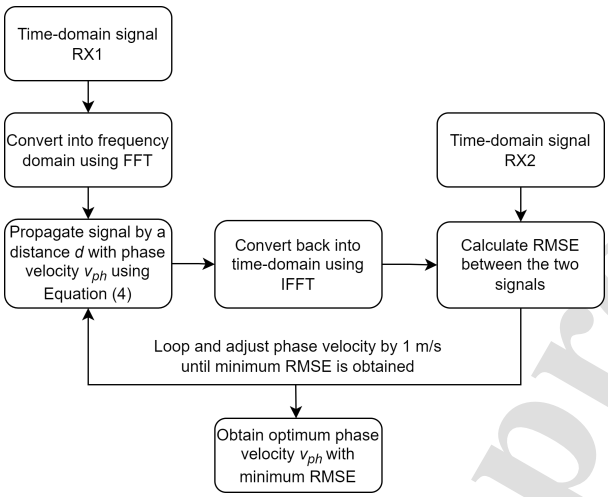

Figure 7: Block diagram process of obtaining phase velocity from guided wave measurements.

properties are not known. However, a curve of best fit was plotted using the following equation

$$c_l = c_o \sqrt{\frac{1 + \alpha_1\ \alpha_2\ k^2}{1 + \alpha_1\ k^2}}, \tag{9}$$

where c_o is the rod velocity, α_1 and α_2 are constants and k is the wavenumber. The optimum values for c_o, α_1 and α_2 were obtained using a non-linear least squares fitting technique. The above equation is based on the correction of the Rayleigh-Bishop theory [39] which approximates the dispersion relation of the fundamental longitudinal wave mode for isotropic bars of any cross-section. The equation was chosen as it is easy to use and gives good approximations at low frequencies.

Using the theoretical and fitted dispersion curves, dispersion compensation was performed on both the simulated and experimental waveforms for the transmitted frequency range using the method described in Section 2. The ToF acoustic velocities were then obtained using the FToA amplitude threshold method. These ToF measurements were obtained both before and after dispersion compensation had been applied to the signals.

3.7. Numerical simulation

Simulations were also performed to evaluate if dispersion was causing any overestimation in amplitude threshold ToF velocity measurements. The advantage of performing these simulations was that it allowed the effects of dispersion to be evaluated without any other external factors being present that could influence the wave propagation.

Two types of excitation signals were used in the simulations. A hammer hit excitation signal was approximated as half of a cycle of a sine wave with frequencies respectively of 2 and 8 kHz for wood and

aluminium samples. These were chosen as the shape was similar to the first cycle of the measured hammer hit signals for these samples. Additionally, a five cycle 15 kHz sine wave was also used.

Using the experimentally measured L(0,1) phase velocity dispersion curves for aluminium and wood, Equation 4 was then used to simulate the propagation of these excitation signals at a distance of 2510 mm for both samples respectively. Figure 8 shows an example of the simulated transmitted and received signals for the aluminium sample.

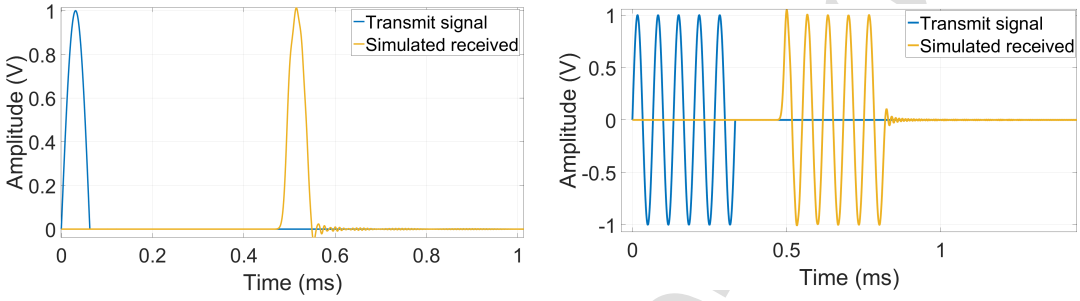

(a) Half a cycle of a 8 kHz sine wave.

(b) Five cycles of a 15 kHz sine wave.

Figure 8: Plots showing the simulated transmit and received signal using different signal excitation for the aluminium sample.

The FToA of the received signals were then determined from the simulated signals using the amplitude threshold method with a threshold value of 0.01 V. The simulated amplitude threshold ToF acoustic velocity was then measured using Equation 3.

4. Results

Table 1 shows the experimental acoustic velocities obtained using resonance, amplitude threshold ToF and guided wave methods for both aluminium and wood samples, before any dispersion compensation was performed. Note that the resonance and hammer hit ToF acoustic velocities presented in the table are obtained from the average of five measurements. Both tone burst and guided wave measurements produced similar results for each individual recording hence the uncertainty of the two measurements was calculated from the sampling resolution. Results from the table show that the acoustic velocities obtained using the amplitude threshold ToF(for both hammer hit and tone burst excitation) and guided waves method were higher than resonance. This is observed for both the aluminium and wood samples. The ToF velocity measurements were outside the uncertainty range for resonance and were approximately 1.8 - 3.2% higher. Guided wave velocities have a lower overestimation ($< 1\%$) relative to resonance and are within the uncertainty of the resonance velocity measurements.

Note that the measured acoustic velocities for the aluminium sample are significantly lower than the expected bulk wave speed of 6175 m/s. This indicates that bulk waves were not being measured and hence

Table 1: Experimental acoustic velocity measurements obtained using different excitation methods for the aluminium and wood samples. The guided wave acoustic velocity represents the phase velocity of a 5 cycle Hanning-windowed 15 kHz sine wave.

Methods	**Aluminium (m/s)**	**Wood (m/s)**
Resonance	5036 ± 21	4463 ± 41
Hammer (ToF)	5130 ± 35	4592 ± 33
Tone burst (ToF)	5141 ± 7	4608 ± 7
Guided Waves	5062 ± 7	4508 ± 7

this is not a cause of the overestimation relative to resonance observed for this sample.

4.1. Experimental dispersion curves

Figure 9 shows the guided wave phase velocity measurements obtained for the aluminium and wood samples. Each data point in the figure represents a single measurement obtained using a narrowband excitation signal. This excitation signal was composed of five cycles of a Hanning-windowed sine wave with a central frequency f_o. These measurements were repeated using values of f_o which ranged from 15 kHz to 50 kHz for aluminium and 15 kHz to 40 kHz for wood in 1 kHz increments. The frequency range used for the two materials was different due to the higher attenuation rate in wood at higher frequencies. For the wood sample, the phase velocities for frequencies above 40 kHz could not be measured reliably as the received signals were highly distorted due to attenuation and hence the results were omitted. Overlaid are their respective phase velocity dispersion curves. For aluminium, the theoretical dispersion curve was obtained using GUIGUW. For wood, the dispersion curve was obtained by fitting a curve through the guided wave phase velocity measurements using the method described in Section 3.6. Both dispersion curves are observed to match well with the experimental guided wave measurements. The average error between the measured and theoretical/fitted phase velocities were 5 m/s and 7 m/s for aluminium and wood respectively. The fitted dispersion curve for wood has high R^2 value (0.99) at the frequency range of interest. Figure 9 also shows that the dispersion curve for wood has more curvature compared to aluminium which implies that the wood sample is more dispersive.

Figure 10 shows the wavenumber-frequency domain plots which were presented in our previous paper [21] for the same samples. Overlaid are the guided wave phase velocities and dispersion curves shown in Figure 9 which have been converted into wavenumber using Equation 5. It can be seen that the guided wave measurements and dispersion curves matches well with the L(0,1) wave mode from the wavenumber-frequency plots. Note that the wavenumber-frequency domain plots have relatively low resolution. This would cause dispersion curves obtained from the wavenumber-frequency domain plots to high variations when converted to phase velocity-frequency domain compared to dispersion curves obtained directly from phase velocity measurements. The error is more prominent at lower frequencies and decreases with increase

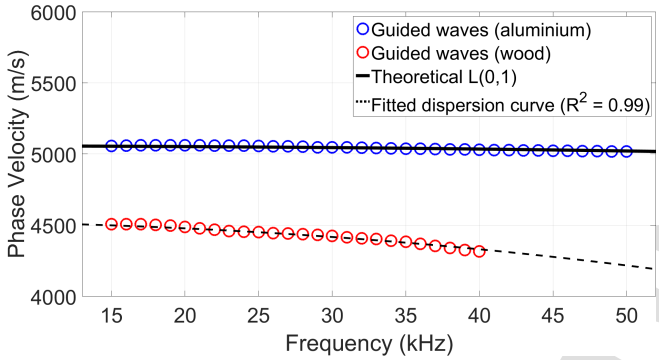

Figure 9: Guided wave phase velocity measurements overlaid with dispersion curves for aluminium and wood sample.

in frequency.

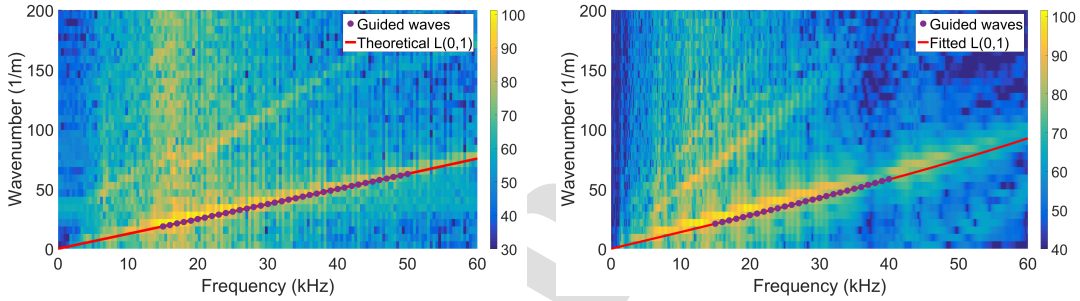

(a) Wavenumber-frequency plot for aluminium

(b) Wavenumber-frequency plot for wood

Figure 10: Wavenumber-frequency plots obtained using the 2D FFT method overlaid with experimental guided wave measurements and fitted dispersion curves.

4.2. Simulated ToF measurements

Simulations were performed using the method described in Section 3.7 to evaluate the effects of dispersion on amplitude threshold ToF measurements and if these effects could be mitigated using dispersion compensation. The received signal at RX1 and RX2 were simulated using the measured dispersion curves of the L(0,1) wave mode shown in Figure 9. Amplitude threshold ToF acoustic velocity measurements were first obtained from the unprocessed simulated signals for the simulated hammer hit and tone burst excitation. Dispersion compensation was then performed in post-processing on the simulated received signal for both RX1 and RX2. Amplitude threshold ToF velocity measurements were then repeated on the dispersion compensated received signals.

Figure 11 shows an example of the simulated received signal for the aluminium sample before and after dispersion compensation has been performed. Note that these plots have been zoomed in to show the first

Table 2: Simulated acoustic velocity measurements for aluminium and wood before and after dispersion compensation. Note that the expected theoretical resonance velocities for aluminium and wood are 5058 and 4526 m/s respectively.

Material	**Excitation**	**Dispersion compensation**	
		Before (m/s)	**After (m/s)**
Aluminium	Hammer	5130	5064
	Tone burst	5141	5072
Wood	Hammer	4592	4538
	Tone burst	4608	4545

arrival of the signal at the RX2 transducer located at the end of the sample, see Figure 5. The plots show that dispersion compensation resulted in a significant difference in rise time at the start of the signal. The dispersion compensated signal has a sharper rise time and is slightly delayed compared to the original signal. However, the phase and rise time were not significantly different at other times. This was also observed for the wood sample. The large difference in rise time at the start of the signal could lead to a difference in amplitude threshold ToF measurement and acoustic velocity measurement of the propagating wave.

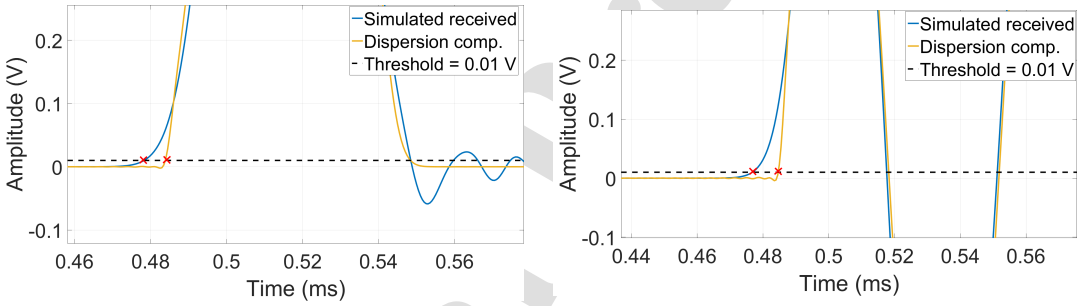

(a) Simulated hammer hit.

(b) Simulated tone burst.

Figure 11: Plots showing the simulated received signal for the transducer RX2 located at the end of the sample before and after dispersion compensation for a half-cycle 8 kHz sine wave, meant to roughly approximate a hammer hit, and a 5 cycle 15 kHz tone burst for aluminium.

The simulated signals were processed using the FToA amplitude threshold method to obtain simulated ToF velocity measurements. The measured amplitude threshold ToF velocities of the simulated signals, before and after dispersion compensation, were obtained for the aluminium and wood samples, see Table 2. The results show that the measured acoustic velocities before dispersion compensation was performed were higher than the expected resonance velocity. The results also show a reduction in the simulated acoustic velocities after dispersion compensation was performed making them closer to the expected theoretical resonance values.

4.3. Experimental ToF measurements

Experimental measurements using hammer hit and tone burst excitations were also performed to investigate the effects of dispersion on amplitude threshold ToF measurements. Figure 12 shows the time-domain and frequency-domain spectra of the experimentally received signal from transducers RX1 and RX2 using hammer hit excitation for the aluminium and wood samples. It be seen that the wood sample has higher attenuation with increased frequency compared to the aluminium sample.

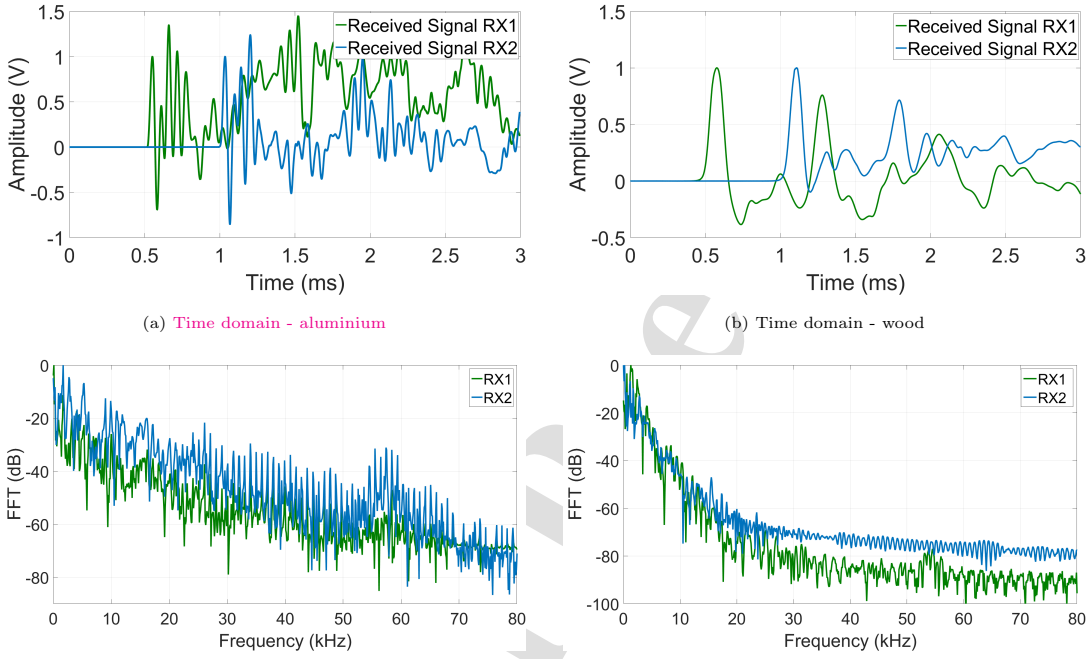

(a) Time domain - aluminium

(b) Time domain - wood

(c) Frequency domain - aluminium

(d) Frequency domain - wood

Figure 12: Plots showing the time-domain and frequency-domain spectra of the received signals at transducers RX1 and RX2 for aluminium and wood samples using hammer hit excitation.

In a similar manner to that used in the simulations, post-processing was performed on the experimental RX1 and RX2 received signals to obtain amplitude threshold ToF measurements. These ToF measurements were obtained both before and after dispersion compensation was performed on the received signals. Figure 13 shows plots of the original received signal and the dispersion compensated signal for the aluminium and wood samples. Note that the arrivals times of the received signal for the hammer hit excitation and tone burst excitation are different as the hammer hit was performed manually without any hardware synchronisation. The results from the figure are similar to what had been observed in the simulations. The plots show that the rise time at the start of the received signal becomes sharper and is slightly delayed for the dispersion compensated signal. Also, the phase and rise time of the received signal before and after disper-

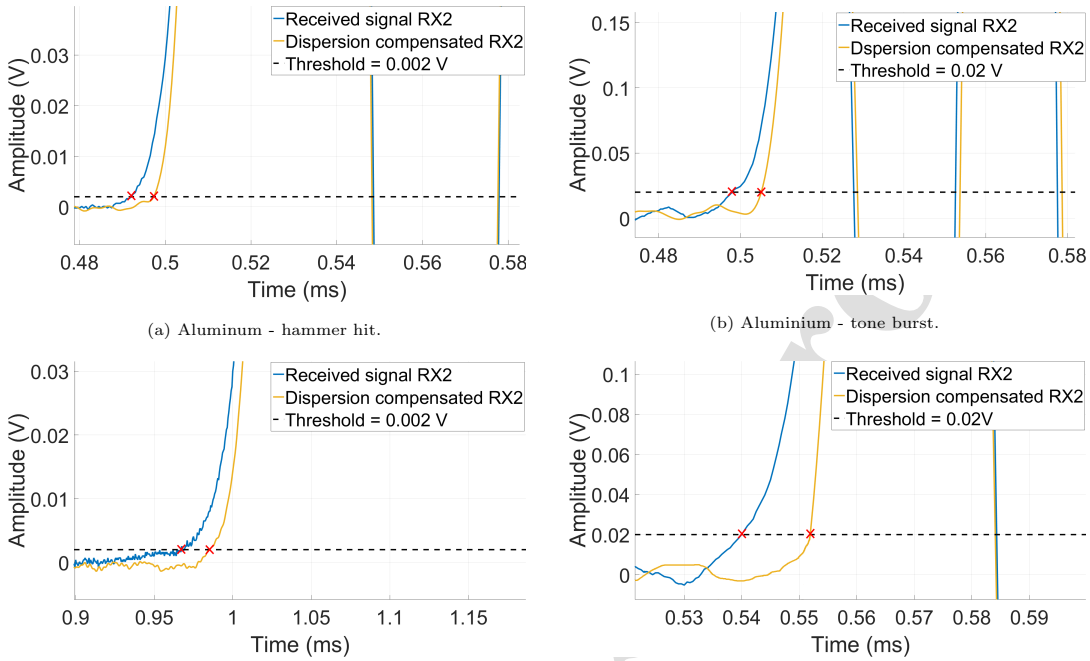

(a) Aluminum - hammer hit.

(b) Aluminium - tone burst.

(c) Wood - hammer hit.

(d) Wood - tone burst.

Figure 13: Plots showing the effect of performing dispersion compensation on experimental ToF measurement signals on transducer RX2 for the aluminum and wood samples using a hammer impact and a 5 cycle 15 kHz sine wave tone burst excitation signal.

sion compensation were similar at other times. This was observed for both the hammer hit and tone burst measurements.

The average acoustic resonance velocity for the aluminium and wood samples are 5036 $\pm$ 21 m/s and 4463 $\pm$ 41 m/s respectively. Table 3 shows the experimental amplitude threshold ToF acoustic velocities measured before and after dispersion compensation was performed on the received signal. The results show that the amplitude threshold ToF measured acoustic velocities for the dispersion compensated signal are smaller than the original dispersed signal and is quite similar to the resonance velocity. This indicates that dispersion compensation was able to reduce the overestimation of the amplitude threshold ToF measurements relative to resonance. Note that the measured acoustic velocity using the tone burst excitation is slightly higher than the hammer impact for both the original and dispersion compensated signal.

Table 3: Experimental amplitude threshold ToF acoustic velocity measurements for aluminium and wood before and after dispersion compensation. Note that the acoustic resonance velocity for the aluminium and wood samples are 5036 ± 21 m/s and 4463 ± 41 m/s respectively.

Material	**Excitation**	**Dispersion compensation**	
		Before (m/s)	**After (m/s)**
Aluminium	Hammer	5130 ± 35	5064 ± 16
	Tone burst	5141 ± 7	5072 ± 7
Wood	Hammer	4592 ± 33	4476 ± 33
	Tone burst	4608 ± 7	4525 ± 7

5. Conclusion

This work investigates the effects of dispersion on ToF acoustic velocity measurements obtained using the amplitude threshold FToA method. This technique uses the very start of the signal to measure the acoustic velocity and is the most common technique used for ToF acoustic velocity measurements in wood.

Acoustic velocity measurements using amplitude threshold ToF, resonance and guided wave methods were performed on 16 mm diameter wood and aluminium rod samples. The guided wave measurements were used to obtain experimental measurements of the phase velocity dispersion curves for the L(0,1) wave mode. These dispersion curves were used to simulate the wave propagation along the rods and to perform dispersion compensation for both the simulated and experimental data. Dispersion compensation was performed to mitigate the effects of dispersion.

Comparisons were made between the received signal before and after performing dispersion compensation for the simulated and experimental data. The results showed that dispersion caused the received signal to spread out as it propagated. This resulted in the signal arriving earlier at the second transducer and having a lower rise time than the dispersion compensated signal. This distortion at the front portion of the dispersed signal resulted in an overestimation of the measured acoustic velocity relative to resonance when using the amplitude threshold FToA technique. Dispersion compensation mitigated this distortion and hence reduced the overestimation, providing ToF acoustic velocity measurements that were closer to the resonance velocities. The L(0,1) wave mode for the aluminium sample had relatively low dispersion. However, the results showed that overestimation in amplitude threshold ToF measurements can still occur at these low dispersion levels. To the best of the authors' knowledge, this is the first study to have shown that dispersion can cause an overestimation in ToF velocity measurements obtained using FToA techniques.

The study showed that dispersion can be a potential cause of the overestimation of ToF acoustic velocity measurements obtained using the FToA amplitude threshold technique. The same effect is expected to occur for other FToA techniques such as AIC and MER since these techniques also utilise the front portion of the received signal. The dispersion compensation technique can be used to mitigate dispersion effects and

reduce the resulting overestimation of the measured ToF acoustic velocity caused by these effects.

For guided wave testing of metal structures, dispersion effects are usually reduced by using narrow bandwidth excitation signals. There have been a couple of studies that have investigated this technique for wood. For example, Subhani et.al [22] investigated ways to reduce the effects of dispersion in timber utility poles using finite element analysis by selecting the optimum excitation frequency. However, the previous studies did not report any FToA acoustic velocity measurements.

The amplitude threshold ToF velocity overestimation observed in this study was relatively low (less than 3%) compared to the values reported in the literature for standing trees, which ranged from about 7 to 31% for radiata pine [4]. However, this study was performed using thin (16 mm diameter) rods, which had relatively minimal dispersion in the excitation frequency range used for the fastest wave mode, the fundamental longitudinal L(0,1) wave mode.

This study has been performed on a small diameter wood sample. For larger diameter samples such as tree stems, higher dispersion would be expected to occur, which could lead to higher overestimations. Further work should be performed on larger diameter samples to investigate the relationship between the measured dispersion curves and any observed overestimation in ToF acoustic velocity relative to resonance. This should include both broadband and narrowband excitation. The experiments should also be repeated on logs, seedlings and standing trees with varying diameters to determine the practicality of the dispersion compensation technique. Other guided wave techniques should also be investigated which can help obtain improved NDT measurements. Stiffness measurements should also be obtained using the techniques in this study and compared with stiffness measurements obtained using static bending test.

References

[1] R. L. Dickson, C. A. Raymond, W. Joe, C. A. Wilkinson, Segregation of *Eucalyptus dunnii* logs using acoustics, Forest Ecology and Management 179 (1-3) (2003) 243–251.

[2] H. Heräjärvi, Static bending properties of Finnish birch wood, Wood Science and Technology 37 (6) (2004) 523–530.

[3] R. Meder, A. Thumm, D. Marston, Sawmill trial of at-line prediction of recovered lumber stiffness by NIR spectroscopy of *Pinus radiata* cants, Journal of Near Infrared Spectroscopy 11 (2) (2003) 137–143.

[4] X. Wang, Acoustic measurements on trees and logs: a review and analysis, Wood Science and Technology 47 (5) (2013) 965–975.

[5] X. Wang, R. J. Ross, P. Carter, Acoustic evaluation of wood quality in standing trees. Part I. Acoustic wave behavior, Wood and Fiber Science 39 (1) (2007) 28–38.

[6] M. Legg, S. Bradley, Measurement of stiffness of standing trees and felled logs using acoustics: A review, The Journal of the Acoustical Society of America 139 (2) (2016) 588–604.

[7] C. R. Mora, L. R. Schimleck, F. Isik, J. M. Mahon, A. Clark, R. F. Daniels, Relationships between acoustic variables and different measures of stiffness in standing pinus taeda trees, Canadian Journal of Forest Research 39 (8) (2009) 1421–1429.

[8] H. Maurer, S. I. Schubert, F. Bächle, S. Clauss, D. Gsell, J. Dual, P. Niemz, A simple anisotropy correction procedure for acoustic wood tomography (2006).

[9] K. T. Hassan, P. Horáček, J. Tippner, Evaluation of stiffness and strength of scots pine wood using resonance frequency and ultrasonic techniques, BioResources 8 (2) (2013) 1634–1645.

[10] F. Liu, P. Xu, H. Zhang, C. Guan, D. Feng, X. Wang, Use of time-of-flight ultrasound to measure wave speed in poplar seedlings, Forests 10 (8) (2019) 682.

[11] M. Kaphle, A. C. Tan, D. P. Thambiratnam, T. H. Chan, Identification of acoustic emission wave modes for accurate source location in plate-like structures, Structural control and health monitoring 19 (2) (2012) 187–198.

[12] S. Y. Chong, J.-R. Lee, C. Y. Park, Statistical threshold determination method through noise map generation for two dimensional amplitude and time-of-flight mapping of guided waves, Journal of Sound and Vibration 332 (5) (2013) 1252–1264.

[13] X. Wang, F. Divos, C. Pilon, B. K. Brashaw, R. J. Ross, R. F. Pellerin, Assessment of decay in standing timber using stress wave timing nondestructive evaluation tools: A guide for use and interpretation, Gen. Tech. Rep. FPL-GTR-147. Madison, WI: US Department of Agriculture, Forest Service, Forest Products Laboratory, 2004. 12 pages 147 (2004).

[14] L. Espinosa, J. Bacca, F. Prieto, P. Lasaygues, L. Brancheriau, Accuracy on the time-of-flight estimation for ultrasonic waves applied to non-destructive evaluation of standing trees: A comparative experimental study, Acta Acustica united with Acustica 104 (3) (2018) 429–439.

[15] L. Han, J. Wong, J. Bancroft, et al., Time picking and random noise reduction on microseismic data, CREWES Research Report 21 (2009) 1–13.

[16] G. Emms, B. Nanayakkara, J. Harrington, A novel technique for non-damaging measurement of sound speed in seedlings, European Journal of Forest Research 131 (5) (2012) 1449–1459.

[17] A. Krauss, J. Kúdela, Ultrasonic wave propagation and Young's modulus of elasticity along the grain of Scots pine wood (*Pinus sylvestris L.*) varying with distance from the pith, Wood Research 56 (4) (2011) 479–488.

[18] J. L. Rose, Ultrasonic guided waves in solid media, Cambridge University Press, 2014.

[19] I. A. Veres, M. B. Sayir, Wave propagation in a wooden bar, Ultrasonics 42 (1-9) (2004) 495–499.

[20] S. Dahmen, H. Ketata, M. H. B. Ghozlen, B. Hosten, Elastic constants measurement of anisotropic olivier wood plates using air-coupled transducers generated Lamb wave and ultrasonic bulk wave, Ultrasonics 50 (4-5) (2010) 502–507.

[21] A. H. A. Bakar, M. Legg, D. Konings, F. Alam, Ultrasonic guided wave measurement in a wooden rod using shear transducer arrays, Ultrasonics 119 (2022) 106583.

[22] M. Subhani, J. Li, B. Samali, K. Crews, Reducing the effect of wave dispersion in a timber pole based on transversely isotropic material modelling, Construction and Building Materials 102 (2016) 985–998.

[23] J. El Najjar, S. Mustapha, Understanding the guided waves propagation behavior in timber utility poles, Journal of Civil Structural Health Monitoring 10 (5) (2020) 793–813.

[24] U. Lindholm, Some experiments with the split Hopkinson pressure bar, Journal of the Mechanics and Physics of Solids 12 (5) (1964) 317–335.

[25] D. Gorham, A numerical method for the correction of dispersion in pressure bar signals, Journal of Physics E: Scientific Instruments 16 (6) (1983) 477.

[26] D. Gorham, P. Pope, J. E. Field, An improved method for compressive stress-strain measurements at very high strain rates, Proceedings of the Royal Society of London. Series A: Mathematical and Physical Sciences 438 (1902) (1992) 153–170.

[27] A. Tyas, D. J. Pope, Full correction of first-mode Pochammer–Chree dispersion effects in experimental pressure bar signals, Measurement Science and Technology 16 (3) (2005) 642.

[28] A. Barr, S. Rigby, M. Clayton, Correction of higher mode Pochhammer–Chree dispersion in experimental blast loading measurements, International Journal of Impact Engineering 139 (2020) 103526.

[29] P. D. Wilcox, A rapid signal processing technique to remove the effect of dispersion from guided wave signals, IEEE Transactions on Ultrasonics, Ferroelectrics, and Frequency Control 50 (4) (2003) 419–427.

[30] B. Xu, L. Yu, V. Giurgiutiu, Lamb wave dispersion compensation in piezoelectric wafer active sensor phased-array applications, in: Health Monitoring of Structural and Biological Systems 2009, Vol. 7295, International Society for Optics and Photonics, 2009, p. 729516.

[31] M. Legg, M. K. Yücel, V. Kappatos, C. Selcuk, T.-H. Gan, Increased range of ultrasonic guided wave testing of overhead transmission line cables using dispersion compensation, Ultrasonics 62 (2015) 35–45.

[32] B. Xu, L. Yu, V. Giurgiutiu, Advanced methods for time-of-flight estimation with application to Lamb wave structural health monitoring, in: Proc. International Workshop on SHM, 2009, pp. 1202–1209.

[33] R. Sicard, J. Goyette, D. Zellouf, A numerical dispersion compensation technique for time recompression of Lamb wave signals, Ultrasonics 40 (1-8) (2002) 727–732.

[34] K. Xu, D. Ta, P. Moilanen, W. Wang, Mode separation of Lamb waves based on dispersion compensation method, The Journal of the Acoustical Society of America 131 (4) (2012) 2714–2722.

[35] P. Bocchini, A. Marzani, E. Viola, Graphical User Interface for Guided Acoustic Waves, Journal of Computing in Civil Engineering 25 (3) (2011) 202–210.

[36] B. A. Engineer, The mechanical and resonant behaviour of a dry coupled thickness-shear PZT transducer used for guided wave testing in pipe line, Ph.D. thesis, Brunel University (2013).

[37] M. Legg, S. Bradley, Experimental measurement of acoustic guided wave propagation in logs, in: 19th International Nondestructive Testing and Evaluation of Wood Symposium, Rio de Janeiro, Brazil, 2015, pp. 681–688.
URL https://www.fs.usda.gov/treesearch/pubs/49713

[38] D. Brizard, An impact test to determine the wave speed in shpb: Measurement and uncertainty, Journal of Dynamic Behavior of Materials 6 (1) (2020) 45–52.

[39] G. Carta, Correction to Bishop's approximate method for the propagation of longitudinal waves in bars of generic cross-section, European Journal of Mechanics-A/Solids 36 (2012) 156–162.

Highlights

- Resonance, ToF and guided waves velocity measurements for wood and aluminium rods
- Dispersion observed to be a potential cause of the ToF velocity overestimation
- Dispersion compensation used to mitigate ToF velocity overestimation

Declaration of interests

☒ The authors declare that they have no known competing financial interests or personal relationships that could have appeared to influence the work reported in this paper.

☐ The authors declare the following financial interests/personal relationships which may be considered as potential competing interests: